

ChemComm

Accepted Manuscript



This is an *Accepted Manuscript*, which has been through the Royal Society of Chemistry peer review process and has been accepted for publication.

Accepted Manuscripts are published online shortly after acceptance, before technical editing, formatting and proof reading. Using this free service, authors can make their results available to the community, in citable form, before we publish the edited article. We will replace this *Accepted Manuscript* with the edited and formatted *Advance Article* as soon as it is available.

You can find more information about *Accepted Manuscripts* in the [Information for Authors](#).

Please note that technical editing may introduce minor changes to the text and/or graphics, which may alter content. The journal's standard [Terms & Conditions](#) and the [Ethical guidelines](#) still apply. In no event shall the Royal Society of Chemistry be held responsible for any errors or omissions in this *Accepted Manuscript* or any consequences arising from the use of any information it contains.

COMMUNICATION

Synthesis of U_3Se_5 and U_3Te_5 type polymorphs of Ta_3N_5 by combining high pressure–temperature pathways with a chemical precursor approach

Cite this: DOI: 10.1039/x0xx00000x

Received 00th January 2012,

Accepted 00th January 2012

DOI: 10.1039/x0xx00000x

www.rsc.org/

Ashkan Salamat,^{*,a} Katherine Woodhead,^b S. Imran U. Shah,^c Andrew L. Hector^{*,c} and Paul F. McMillan^{*,c}

Combining metastable precursors with high pressure–temperature treatment is a powerful tool to make nitrogen-rich metal nitrides. Two new dense polymorphs of Ta_3N_5 have previously been theoretically predicted, with U_3Se_5 (*Pnma*) and U_3Te_5 (*Pnma*) structure types, and are now shown to exist. Amorphous Ta_3N_5 from thermal ammonolysis of an amorphous polymeric precursor was laser heated at 22 GPa and examined using synchrotron X-ray diffraction to reveal the emergence of these two novel polymorphs.

The maximum observed metal oxidation state in transition metal nitrides is typically lower than that found in the oxides.¹ Prior to 2003 Ta_3N_5 and Zr_3N_4 were the only well characterized examples of nitride compounds with the metal in its maximum oxidation state, as these phases form via elevated temperature reactions of the metal chloride (Ta and Zr) or oxide (Ta) with ammonia.^{2–5} Unlike metallic lower nitrides these compounds are semiconductors giving rise to optoelectronic applications. For example Ta_3N_5 is an orange-red pigment⁶ that has been extensively studied for its visible light photocatalytic activity.^{7–9}

The application of synthesis in diamond anvil cells (DACs) to high oxidation state transition metal nitrides was first described by Zerr *et al.*, who used laser heating (LH) to combine elemental Zr and Hf with nitrogen at high pressure and obtain the Th_3P_4 -type Zr_3N_4 and Hf_3N_4 phases.¹⁰ The cubic Zr_3N_4 polymorph has extremely high hardness and has since been produced by thin film techniques.¹¹ Analogous methods have since been applied to obtain W_2N_3 , W_3N_4 ,¹² ReN_2 ¹³ and the first platinum group metal nitrides.^{14–17} It is important to develop the solid state chemistry of such high oxidation state nitrides in our search for new materials with important electronic and high hardness properties.

The tantalum–nitrogen system includes the subnitride Ta_2N , several TaN polymorphs, Ta_5N_6 , Ta_4N_5 , Ta_2N_3 and Ta_3N_5 .¹ Density-functional theory (DFT) calculations by Kroll *et al.* have predicted that the known *Cmcm* Ta_3N_5 -I semiconducting phase should transform into a metallic Ta_3N_5 -II polymorph with the U_3Te_5 structure at ~10 GPa.¹⁸ A second U_3Se_5 structured phase lies at similar energy at this pressure and a further transformation into the Sm_2SnS_5 structure type could occur above 20 GPa (Fig. 1).¹⁸ Previous attempts to obtain these phases by high pressure–high temperature synthesis from the elements or Ta_3N_5 have only succeeded in producing Ta_2N_3 .^{19,20} Here we report the first evidence of U_3Se_5 - and U_3Te_5 -structured Ta_3N_5 using LH-DAC techniques combined with a chemical precursor approach.

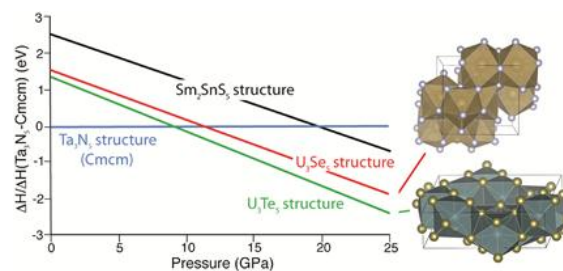
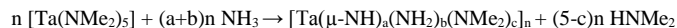


Fig. 1 Calculated enthalpy–pressure relationship between different possible Ta_3N_5 polymorphs normalized to the enthalpy of the ambient pressure phase (redrawn from ref 18), and structures of the two structure types predicted to be most stable at elevated pressure.

Reactions of metal dialkylamides with ammonia result in polymeric precipitates that can be pyrolysed to make nitrides or carbonitrides.^{21–23} Controlling the decomposition process results in highly nitrated amorphous or nanocrystalline materials that can offer access to higher oxidation state compounds than other synthesis

approaches. In our recent synthesis of two high pressure Hf_3N_4 polymorphs we took a nanocrystalline Hf_3N_4 material made by pyrolysis of such a polymer in ammonia, and laser heated it under pressure to produce new crystalline phases identified by synchrotron XRD.²⁴ Solution phase reactions of $\text{Ta}(\text{NMe}_2)_5$ with ammonia proceed via transamination and condensation to produce a polymeric solid with variable amounts of bridging imide, terminal amide and terminal dimethylamide groups:^{21,22}



Firing the yellow precipitate in ammonia resulted in broad diffraction features at lower temperatures followed by crystallisation of the known *Cmcm* phase of Ta_3N_5 at 800 °C (Fig. 2). Rietveld fitting of this pattern shows the material to be identical to that produced conventionally by ammonolysis of Ta_2O_5 . The UV-visible spectrum of this maroon-coloured sample (Fig. 2) shows an absorption edge at ~600 nm corresponding to an optical band gap of 2.07 eV (2.08 eV for Ta_3N_5 obtained from Ta_2O_5).⁴ The broad X-ray feature between ~25-40° 2 θ (maximum near $d = 2.71$ Å) observed for samples made at 500-700 °C indicates amorphous material.

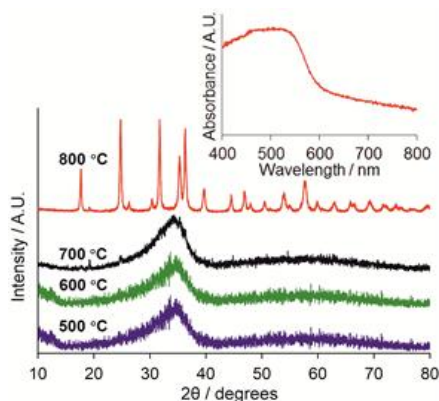


Fig. 2 PXD patterns ($\lambda = 1.5406$ Å) of the tantalum nitrides obtained by firing the polymer precursor under ammonia at various temperatures. The reflections observed after firing at 800 °C match those expected for the *Cmcm* phase of Ta_3N_5 . Inset: The UV-visible spectrum of crystalline- Ta_3N_5 obtained by firing the polymer precursor under ammonia at 800 °C.

Combustion analysis of the crystalline Ta_3N_5 sample produced at 800 °C showed 11.5% N (theoretical 11.4% for stoichiometric Ta_3N_5) with no C or H (<0.1%) present. Samples heated at 500, 600 and 700 °C contained 0.8-0.9% C, no H and 12.3 (500 °C), 12.9 (600 °C) or 13.5% (700 °C) nitrogen. Thermogravimetric analyses showed negligible (<0.2%) mass loss, indicating that all or most amide/imide groups present in the starting amorphous polymer had decomposed by these temperatures. All samples decreased in weight above ~750 °C due to nitrogen loss as observed for crystalline Ta_3N_5 transforming to TaN.

The 500 °C Ta_3N_5 amorphous precursor sample was chosen for high pressure-high temperature studies as similar compositions were obtained at all temperatures and local order was likely to be minimized at the lowest annealing temperature. The broad main diffraction feature moves to slightly higher d -spacing on initial compression, before steadily decreasing above ~5 GPa. This is consistent with an initial coordination increase in the densified amorphous material followed by general shortening of the Ta-N bond lengths with pressure. The sample was then heated at 20 GPa at

~1500-2000 K for several minutes using a CO_2 laser²⁵ before the XRD pattern was collected *ex situ* at ambient temperature. A series of sharp crystalline peaks had replaced the broad amorphous pattern (Fig. 3). Initial crystallographic examination strongly indicated the presence of the predicted U_3Se_5 phase and a series of Rietveld refinements was carried out to test the likely presence of other candidate structures, using literature lattice parameters where these were known in this pressure range (key fits shown in supplementary information).

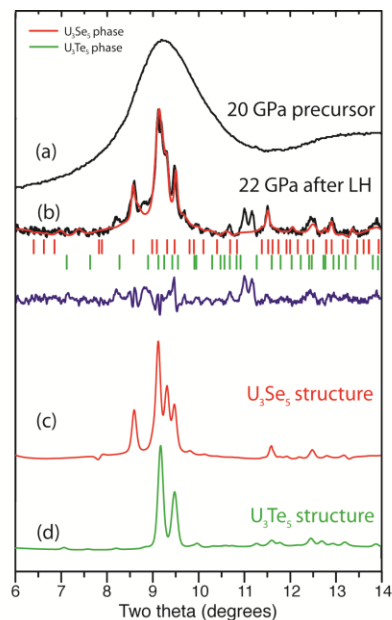


Fig. 3 XRD patterns ($\lambda = 0.411$ Å) of (a) amorphous Ta_3N_5 at 20 GPa (the broad feature is centred on $d = 2.56$ Å at this pressure) and (b) crystalline tantalum nitride after laser heating at 1500-2000 K and 22 GPa. The Rietveld fit to the data (upper black line) after laser heating is shown in red, and the difference plot as the lower black line ($R_{\text{wp}} = 23.39\%$ and $R_p = 19.80\%$). The red tick marks and XRD trace (c) show the allowed reflection positions and refined profile of the U_3Se_5 phase of Ta_3N_5 (*Pnma*, $a = 8.802(3)$, $b = 6.044(4)$ and $c = 5.492(3)$ Å). The green tick marks and XRD trace (d) show the same information for the U_3Te_5 -type phase (*Pnma*, $a = 9.944(2)$, $b = 2.691(6)$ and $c = 9.015(6)$ Å).

Neither the known ambient pressure (*Cmcm*) Ta_3N_5 -I phase nor the Sm_2SnS_5 phase which Kroll predicted to be the third most stable (Fig. 1) yielded a good fit to the data. The major peaks were also not consistent with the decomposition of the sample to the lower nitride compositions of TaN or $\eta\text{-Ta}_2\text{N}_3$. The best fit to a single phase was obtained using the U_3Se_5 -structured phase, and the U_3Te_5 form was the only secondary phase that could fit the shoulder on the right-hand side of the most intense peak at 9.3° . Hence our structural characterisation at ambient temperature following high P,T transformation confirms the presence of the two lowest energy phases predicted by Kroll to exist between 10-20 GPa.¹⁸ The U_3Se_5 - and U_3Te_5 -type structures are present in approximately equal amounts and the unit cell parameters correspond closely with DFT predictions.¹⁸ Both the predicted U_3Se_5 and U_3Te_5 phases are calculated to become stabilized above ~10 GPa and remain close in energy throughout the 10-20 GPa range (Fig. 1) so that the simultaneous presence of both polymorphs following high pressure-high temperature synthesis is to be expected. Atom positions were taken from the known U_3Se_5 and U_3Te_5 structures^{26,27} and were not refined further due to the limited 2θ range and overlapping patterns

present in the data set. Only peak shape and lattice parameters were refined for the U_3Se_5 phase, whereas a spherical harmonic preferred orientation model was used to fit U_3Te_5 .

Previous attempts to synthesize the high-density Ta_3N_5 polymorphs applied LH-DAC to elemental Ta + N_2 at 2000 K and up to 27 GPa²⁰ or multianvil high-P,T treatment of Ta_3N_5 at 1800-2000 K and 9-11 GPa.¹⁹ Both approaches resulted in formation of the lower nitride phase η - Ta_2N_3 . The P,T conditions of most of these experiments lie within the stability range of Ta_2N_3 predicted by Kroll,^{1,28} although Friedrich's²⁰ highest pressure experiments lie close to the Ta_3N_5 -II stability boundary according to Kroll's calculations. Close examination of our data reveals that a small amount of η - Ta_2N_3 is in fact present along with a small amount of ϵ - N_2 , produced by thermal decomposition of the Ta_3N_5 starting material along with the high P,T crystallisation into U_3Se_5 - and U_3Te_5 -structured phases (Fig. 4). Le Bail fitting of these additional phases reveals lattice parameters of $a = 8.082(5)$, $b = 8.051(5)$ and $c = 2.934(8)$ Å for η - Ta_2N_3 , and $a = 7.323(6)$ and $c = 9.894(5)$ Å for ϵ - N_2 , both consistent with expectations for these phases at the pressures used.^{32,33}

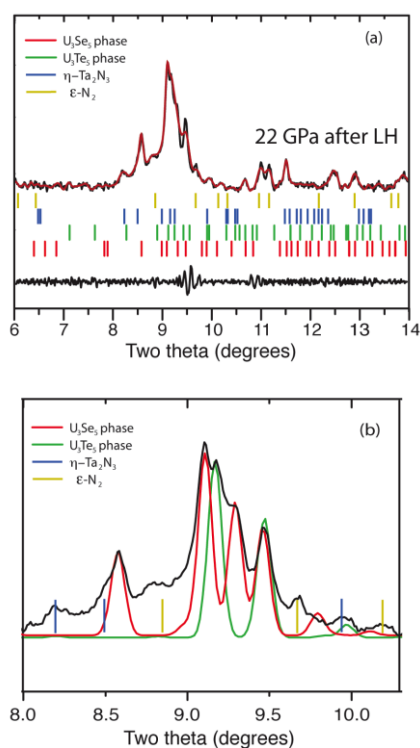


Fig. 4 (a) 4-phase Rietveld fit incorporating η - Ta_2N_3 ($Pbnm$ ³²) and ϵ - N_2 ($R-3c$ ³³) ($R_{wp} = 3.86\%$ and $R_p = 2.75\%$) and (b) expanded plot of XRD data showing the locations of additional peaks not fitted in Fig. 3 compared with positions of the non-zero intense reflections of η - Ta_2N_3 and ϵ - N_2 .

Our synthesis experiments were conducted inside the closed LH-DAC environment using a chemically-produced amorphous precursor with the target stoichiometry and this appears to have been important in achieving the first synthesis of these theoretically predicted phases. Considering the calculated Ta_3N_5 -II stability field²⁸ and the low level of decomposition to η - Ta_2N_3 , it is likely that the temperature experienced by the main part of the sample during our laser heating process was at the lower end of the 1500-2000 K range that we have estimated for the experiment. It is not yet possible to

determine the relative stability relations between the U_3Se_5 - and U_3Te_5 -structured forms because of their closely overlapping enthalpy-pressure relations. In our experiments both were obtained simultaneously. However delicate tuning of the amorphous precursor along with precise control over the P,T synthesis conditions might selectively produce the U_3Se_5 and U_3Te_5 phases. The first order nature of the phase transitions indicates that these structures could be recoverable to ambient conditions although that could not be investigated here due to experimental constraints.

The high pressure-high temperature crystallisation of an amorphous/nanocrystalline Ta_3N_5 precursor results in the first synthesis of two new high-density crystalline polymorphs. These were predicted to exist theoretically but had not been achieved previously using approaches including high-P,T synthesis from the elements or low pressure phases. Our approach represents a versatile technique that can be applied to obtain other highly nitrided compounds with the metals in high oxidation states and high coordination numbers. The previous theoretical investigation indicated that the high pressure Ta_3N_5 -II phases should have metallic properties.¹⁸ This is in agreement with the high optical reflectivity and lack of obvious Raman features observed experimentally (see Supplementary Information). That would make it unsuitable for photocatalysis applications but the conducting powders could have catalytic properties, as found for other transition metal nitrides including MoN.²⁹ Furthermore, the theoretically calculated bulk modulus of the Ta_3N_5 with the U_3Te_5 structure type of 378 GPa describes a highly incompressible material with potentially useful mechanical applications.¹⁸

The authors thank Diamond Light Source for access to beam line I15 (EE986-1) and Dr Heribert Wilhelm for assistance with data collection. KEW, AS and PFM acknowledge support from the Engineering and Physical Sciences Research Council.

Notes and references

^a Lyman Laboratory of Physics, Harvard University, Cambridge, MA 02138, USA.

^b Department of Chemistry, Christopher Ingold Laboratory, University College London, London WC1H 0AJ, UK.

^c Chemistry, University of Southampton, Southampton SO17 1BJ, UK.

† Brief experimental details: A polymeric precursor to Ta_3N_5 was obtained from $Ta(NMe_2)_5$ and ammonia similarly to a previous report.²² The sample was then fired under dry flowing ammonia at 500, 600, 700 or 800 °C for 2h. Powder X-ray diffraction (PXRD) patterns were collected under N_2 with a Siemens D5000 using $Cu-K_{\alpha 1}$ radiation ($\lambda = 1.5406$ Å) and a sample holder for air sensitive material and data were refined using GSAS.³⁰ Combustion analysis of the amorphous Ta_3N_5 precursor was by Medac Ltd. Diffuse reflectance UV-visible spectra were obtained using a Perkin Elmer Lambda 35 spectrometer with an integrating sphere. Raman spectra were recorded using an InVia Renishaw spectrometer with an excitation wavelength 785nm (diode laser) (see ESI). High pressure experiments were carried out in a symmetrical Mao-type cell using brilliant cut type Ia diamonds with 300 μm culets. For pressure measurements, the ruby fluorescence peak was excited by Ar^+ laser radiation of wavelength 514.5 nm. The amorphous precursor was treated as air sensitive and all loadings were carried out in an argon glove box, using dried NaCl as the thermal insulator. Laser heating experiments were carried out at UCL using a CO_2 laser ($\lambda = 10.6$ μm)³¹. Synchrotron X-ray diffraction experiments were conducted at the high pressure beamline I15 of Diamond light Source using 30 keV ($\lambda = 0.411$ Å) X-rays in a 20x20 μm collimated beam. Data were collected using a MAR345 detector, integrated with Fit2D and analysed using GSAS.

Electronic Supplementary Information (ESI) available: Full sample preparation details, infrared spectrum and TGA of the polymer precursor,

TGA traces and TEM images of tantalum nitride samples fired at various temperatures, Rietveld fit to the 800 °C sample, Raman spectra before and after laser heating, XRD of the amorphous sample during compression and full crystallographic results for the mixture of new Ta₃N₅ polymorphs. See DOI: 10.1039/c000000x/

- 1 A. Salamat, A. L. Hector, P. Kroll and P. F. McMillan, *Coord. Chem. Rev.*, 2013, **257**, 2063-2072.
- 2 G. Brauer and J. R. Weidlein, *Angew. Chem. Intl. Ed.*, 1965, **4**, 241-242.
- 3 N. E. Brese, M. O'Keeffe, P. Rauch and F. J. DiSalvo, *Acta Crystallogr. Sect. C*, 1991, **47**, 2291-2294.
- 4 S. J. Henderson and A. L. Hector, *J. Solid State Chem.*, 2006, **179**, 3518-3524.
- 5 M. Lerch, E. Fuglein and J. Wrba, *Z. Anorg. Allg. Chem.*, 1996, **622**, 367-372.
- 6 M. Jansen, E. Guenther and H. P. Letschert, German patent 199 07 618.9, 1999.
- 7 G. Hitoki, A. Ishikawa, T. Takata, J. N. Kondo, M. Hara and K. Domen, *Chem. Lett.*, 2002, **31**, 736-737.
- 8 A. Ishikawa, T. Takata, J. N. Kondo, M. Hara and K. Domen, *J. Phys. Chem. B*, 2004, **108**, 11049-11053.
- 9 M. Higashi, K. Domen and R. Abe, *Energy Environ. Sci.*, 2011, **4**, 4138-4147.
- 10 A. Zerr, G. Miehe and R. Riedel, *Nat. Mater.*, 2003, **2**, 185-189.
- 11 M. Chhowalla and H. E. Unalan, *Nat. Mater.*, 2005, **4**, 317-322.
- 12 S. Wang, X. Yu, Z. Lin, R. Zhang, D. He, J. Qin, J. Zhu, J. Han, L. Wang, H.-K. Mao, J. Zhang and Y. Zhao, *Chem. Mater.*, 2012, **24**, 3023-3028.
- 13 F. Kawamura, H. Yusa and T. Taniguchi, *Appl. Phys. Lett.*, 2012, **100**, 251920-251913.
- 14 E. Gregoryanz, C. Sanloup, M. Somayazulu, J. Badro, G. Fiquet, H. K. Mao and R. J. Hemley, *Nat. Mater.*, 2004, **3**, 294-297.
- 15 J. C. Crowhurst, A. F. Goncharov, B. Sadigh, C. L. Evans, P. G. Morrall, J. L. Ferreira and A. J. Nelson, *Science*, 2006, **311**, 1275-1278.
- 16 A. F. Young, C. Sanloup, E. Gregoryanz, S. Scandolo, R. J. Hemley and H.-K. Mao, *Phys. Rev. Lett.*, 2006, **96**, 155501-155504.
- 17 J. C. Crowhurst, A. F. Goncharov, B. Sadigh, J. M. Zaug, D. Aberg, Y. Meng and V. B. Prakapenka, *J. Mater. Res.*, 2008, **23**, 1-5.
- 18 P. Kroll, T. Schroter and M. Peters, *Angew. Chem. Intl. Ed.*, 2005, **44**, 4249-4254.
- 19 A. Zerr, G. Miehe, J. W. Li, D. A. Dzivenko, V. K. Bulatov, H. Hofer, N. Bolfan-Casanova, M. Fialin, G. Brey, T. Watanabe and M. Yoshimura, *Adv. Funct. Mater.*, 2009, **19**, 2282-2288.
- 20 A. Friedrich, B. Winkler, L. Bayarjargal, E. A. J. Arellano, W. Morgenroth, J. Biehler, F. Schroder, J. Y. Yan and S. M. Clark, *J. Alloys Compds.*, 2010, **502**, 5-12.
- 21 G. M. Brown and L. Maya, *J. Am. Ceram. Soc.*, 1988, **71**, 78-82.
- 22 D. V. Baxter, M. H. Chisholm, G. J. Gama, V. F. DiStasi, A. L. Hector and I. P. Parkin, *Chem. Mater.*, 1996, **8**, 1222-1228.
- 23 A. W. Jackson, O. Shebanova, A. L. Hector and P. F. McMillan, *J. Solid State Chem.*, 2006, **179**, 1383-1393.
- 24 A. Salamat, A. L. Hector, B. M. Gray, A. S. J. Kimber, P. Bouvier and P. F. McMillan, *J. Amer. Chem. Soc.*, 2013, **135**, 9503-9511.
- 25 A. Salamat, K. Woodhead, P. F. McMillan, R. Q. Cabrera, A. Rahman, D. Adriaens, F. Cora and J. P. Perrillat, *Phys. Rev. B*, 2009, **80**, 104106-6.
- 26 O. Tougait, M. Potel and H. J. Noël, *Solid State Chem.*, 1998, **139**, 356-361.
- 27 P. T. Moseley, D. Brown and B. Whittaker, *Acta Crystallogr. Sect. B*, 1972, **28**, 1816-1821.
- 28 P. Kroll, *Mater. Res. Soc. Symp. Proc.*, 2006, 987-991.
- 29 J. S. J. Hargreaves, *Coord. Chem. Rev.*, 2013, **257**, 2015-2031.
- 30 A. C. Larson and R. B. Von Dreele, Los Alamos National Laboratory Report LAUR 2000, 86-748.
- 31 E. Soignard and P. F. McMillan, *Chem. Mater.*, 2004, **16**, 3533-3542.
- 32 J.-D. Zhang and H.-F. Wang, *Physica B: Cond. Matt.*, 2013, **428**, 89-93.
- 33 H. Olijnyk, *J. Chem. Phys.*, 1990, **93**, 8968-8972.